Polarized far-infrared and Raman spectra of Bi_2CuO_4 single crystals

Z V Popović†, G Kliche‡, M J Konstantinović† and A Revcolevschi§

† Institute of Physics, 11000 Belgrade, PO Box 57, Yugoslavia
‡ Max-Planck-Institut für Festkörperforschung, Heisenbergstrasse 1, 7000 Stuttgart 80, Federal Republic of Germany
§ Laboratoire de Chimie des Solides, Unité associée au CNRS 446, Université de Paris-Sud, Bâtiment 414, F-91405 Orsay Cédex, France

Abstract. We present the polarized far-infrared and Raman spectra of Bi_2CuO_4 single crystals at 300 and 10 K in the spectral range from 30 to 650 cm^{-1}. All infrared-active modes ($10E_u + 5A_{2u}$) as well as 21 Raman-active modes were observed. At low temperatures, for $x'y'$ and $x'z$ polarizations, new structure appears which we assigned as a two-magnon mode. The assignment of the observed vibrational modes is given according to Cartesian symmetry coordinates and a preliminary force constant calculation on the basis of a rigid-ion model.

1. Introduction

The discovery of the high-temperature superconducting oxides has led to rapidly increasing interest in studies of the properties of whole series of CuO-based materials. Among the vast group of CuO-based materials, Bi_2CuO_4 attracts extra attention because of its interesting crystal structure and magnetic properties. This oxide has a tetragonal crystal structure [1] with isolated CuO_4 square-planar units of Cu^{2+} ions which are stacked on top of one another in a staggered manner along the c axis.

The magnetic structure of Bi_2CuO_4 is still under investigation. It was shown [2] that Bi_2CuO_4 is an oxide system which exhibits a linear-chain magnetic behaviour. Recently published neutron spectroscopy results of the magnetic structure of Bi_2CuO_4 show [3] that antiferromagnetic ordering in this crystal has 3D character with a tendency to anisotropic 2D magnetic behaviour. Furthermore, there is also some controversy about the spin orientation [4].

In our previously published paper [5] we discussed polarized Raman spectra of Bi_2CuO_4 at 300 K and far-infrared spectra of the ceramic samples. In [6] we reported the measurements of polarized low-temperature Raman spectra of Bi_2CuO_4 single crystals in the spectral range between 10 and 250 cm^{-1} with special attention to one-magnon and two-magnon modes. In this paper we present the polarized far-infrared and Raman spectra of Bi_2CuO_4 single crystals at 300 and 10 K in the spectral range from 10 to 650 cm^{-1}. We observed all infrared-active modes ($10E_u + 5A_{2u}$) as well as 21 Raman-active modes (factor group analysis (FGA) predicts 25 Raman-active modes). The assignment of the observed vibrational modes is given according to Cartesian symmetry coordinates and the preliminary force constant calculation on the basis of a rigid-ion model.

2. Experiment

The crystal growth of Bi_2CuO_4 single crystals was carried out using the floating-zone technique. Polycrystalline feed rods 10 mm in diameter and 80 mm long were prepared by finely grinding Bi_2O_3 and CuO powders, isostatically pressing them under 1 t cm^{-2} in cylindrical rubber tubes and reacting them in air at 750 °C for 24 h. Crystals were grown in air in the [001] direction at a rate of 1 cm h^{-1}, the feed rod and the seed holder being counter-rotated at 30 rev min^{-1}.

The crystals obtained were typically 6–10 mm in diameter and several centimetres long. Growth was frequently perturbed by cracking and cleavage of the crystals along [001] during growth. More details about the crystal growth and properties of samples used in this work can be found in [7].

The Raman spectra were excited by the 514.5 nm line of an argon ion laser (the average power was about 100 mW), focused to a line using a cylindrical lens. The geometry was of a back-scattering nature with an aperture f of the collecting objective of 1:1.4. The monochromator used was U 1000 (Jobin–Yvon, France) with 1800 grooves mm^{-1} holographic gratings. As a detector we used a Pelletier-effect-cooled RCA 31034 A photomultiplier with a conventional photon-counting system. The samples were held in a closed-cycle cryostat (Leybold, Germany), equipped with a low-temperature controller LTC 60 (Leybold) and evacuated by a turbopump.

The polarized far-infrared reflection measurements were measured in the spectral range from 30 to 650 cm^{-1} at both room temperature and liquid-helium temperature using a Bruker (Karlsruhe, Germany) IFS-113v spectrometer with a low-temperature CF 100 cryostat (Oxford, UK).

The single-crystal sample used here was a cylinder 6 mm in diameter and 5 mm long. For $E \perp c$ polarization the high-quality (001) cleavage plane was used. In the case of $E \parallel c$ polarization and also to obtain Raman-active modes of E_g symmetry, the sample was cut along the [001] axis. The surface obtained was then mechanically polished using aqueous suspensions of Al_2O_3 (size, 0.3 μm) on polishing cloths. The orientation of the principal axes was obtained by conventional Laue photographs.

3. Results and discussion

The room-temperature far-infrared reflectivity spectra of Bi_2CuO_4 in the spectral range from 30 to 650 cm^{-1} are given in figure 1. The open circles are experimental data and the full curves are the spectra computed using the four-parameter model for the dielectric constant:

$$\epsilon = \epsilon_\infty \prod_{j=1}^{n} \frac{\omega_{LO,j}^2 - \omega^2 + i\gamma_{LO,j}\omega}{\omega_{TO,j}^2 - \omega^2 + i\gamma_{TO,j}\omega} \tag{1}$$

where $\omega_{TO,j}$ and $\omega_{LO,j}$ are the transverse and longitudinal frequencies of the jth oscillator, $\gamma_{TO,j}$ and $\gamma_{LO,j}$ are their corresponding dampings and ϵ_∞ is the high-frequency dielectric constant. The best-oscillator-fit parameters are listed in table 1. The static dielectric constant, given in table 1, is obtained using the generalized Lyddane–Sachs–Teller (LST) relation

$$\epsilon_0 = \epsilon_\infty \prod_{j=1}^{n} \frac{\omega_{LO,j}^2}{\omega_{TO,j}^2}. \tag{2}$$
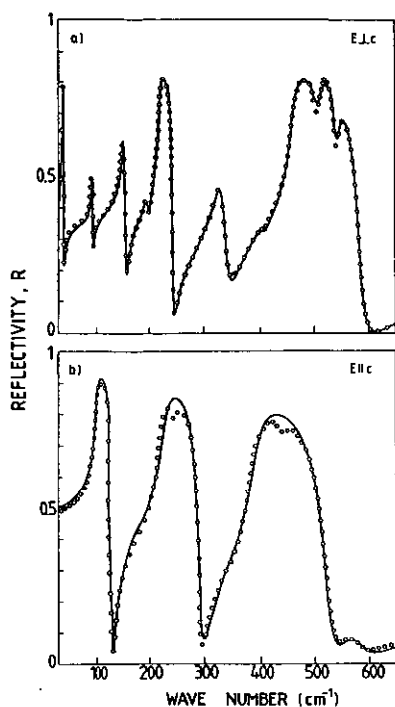
Figure 1. Room-temperature far-infrared reflectivity spectra of Bi_2CuO_4 single crystals for (*a*) $E \perp c$ and (*b*) $E \parallel c$ polarization in the spectral range from 30 to 650 cm^{-1}: O, experimental data; ——, calculated spectra obtained by a fitting procedure based on the model described by equation (1) with the parameter values given in table 1.
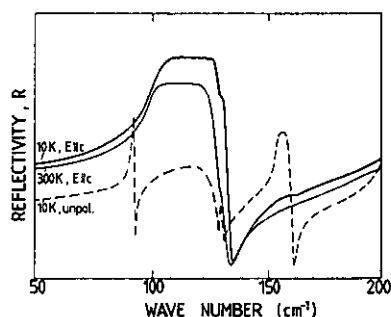
Figure 2. Far-infrared reflectivity spectra of Bi_2CuO_4 in the 50–200 cm^{-1} spectral range.

The FGA [4] for the $P4/ncc$ space group (table 2) gives 15 infrared-active modes: $10E_u + 5A_{2u}$. The E_u-symmetry modes, obtained for $E \perp c$ polarization, are presented in figure 1(*a*). All modes of this polarization were clearly observed. The room-temperature reflectivity spectra for $E \parallel c$ polarization (A_{2u} modes) are shown in figure 1(*b*). Only four oscillators are clearly observed. The fifth oscillator, located at about 130 cm^{-1}, is resolved in figure 2 where reflectivity spectra were measured in the spectral range 50–200 cm^{-1}. The infrared mode at 130 cm^{-1} is observed as a saddle point at room temperature, while at 10 K that mode was much better resolved, which is especially evident for ceramic samples at 10 K (broken curve in figure 2) [5]. Also, good agreement between computed spectra and experimental data (figure 1(*b*)) could not be obtained without this mode.

Polarized Raman spectra of Bi_2CuO_4 in the spectral range between 10 and 650 cm^{-1} at a temperature of 10 K are shown in figure 3. The $5A_{1g}$ and $4B_{2g}$ Raman-active modes, predicted by FGA, are clearly seen in figure 3(*a*). The frequencies of these modes are collected in table 1. Comparing these spectra with our previously published room-temperature results [5] we concluded that the spectra are in agreement except for the A_{1g} mode observed in [5] at 50 cm^{-1}. We believe that this mode could originate from Bi_2O_3 (which remained non-reacted in the sample

Table 1. Infrared (300 K) and Raman (10 K) phonon frequencies of Bi_2CuO_4.

	ω_{TO} (cm^{-1})	γ_{TO} (cm^{-1})	ω_{LO} (cm^{-1})	γ_{LO} (cm^{-1})	ϵ_0	ϵ_∞
A_{2u}	101	6	131	8		
	131	7	132.5	2		
	228	15	293	12	32.8	6
	392	25	525	28		
	560	53	580	60		
E_u	36.8	0.8	39.8	2		
	90.4	2	91.7	2.3		
	149.8	7	157.8	5.6		
	196.5	7	197.5	5.8		
	218	6	244	6.5	16.5	5.5
	324	20.5	342	20		
	402.5	16	404	16		
	461	16	506	21		
	508	18	539	17		
	541.5	17	586	19		
A_{1g}	128	B_{1g}	141	B_{2g}	82	E_g	111
	135		291		132		129
	264		458		287		192
	411		567		474		289
	594						318
							414
							457
							587

Table 2. Factor group analysis of Bi_2CuO_4 ($P4/ncc$ (D_{4h}^8)): S, silent mode; R, Raman-active mode; IR, infrared-active mode.

Atom	Symmetry position	A_{1g}	A_{2g}	B_{1g}	B_{2g}	E_g	A_{1u}	A_{2u}	B_{1u}	B_{2u}	E_u
Cu	4c (C_4)	1	1			2	1	1			2
Bi	8f (C_2)	1	2	2	1	3	1	2	2	1	3
O	16g (C_1)	3	3	3	3	6	3	3	3	3	6
Bi_2CuO_4	Γ_{tot}	5	6	5	4	11	5	6	5	4	11
	Γ_{vib}	5	6	5	4	11	5	5	5	4	10
	Γ_{opt}	5		5	4	11		5			10
	Activity	R	S	R	R	R	S	IR	S	S	IR

used in [5]) because the strongest Raman-active mode of Bi_2O_3 is at about 50 cm^{-1} and it has a very strong Raman scattering cross section [8] for the laser line used.

The A_{1g} mode at 128 cm^{-1} was not resolved in [5] because we used xx polarization which allows observation of the A_{1g} and B_{2g} modes. Since the B_{2g} mode at 132 cm^{-1} is located between two A_{1g} modes, together they form one strong wide mode, and we are not able to observe them separately. Moreover, decomposition of these modes was not possible owing to the limited resolution of the Mepsicron detector system used in [5].

Assignment of the Raman-active modes of Bi_2CuO_4 and their normal coordinates
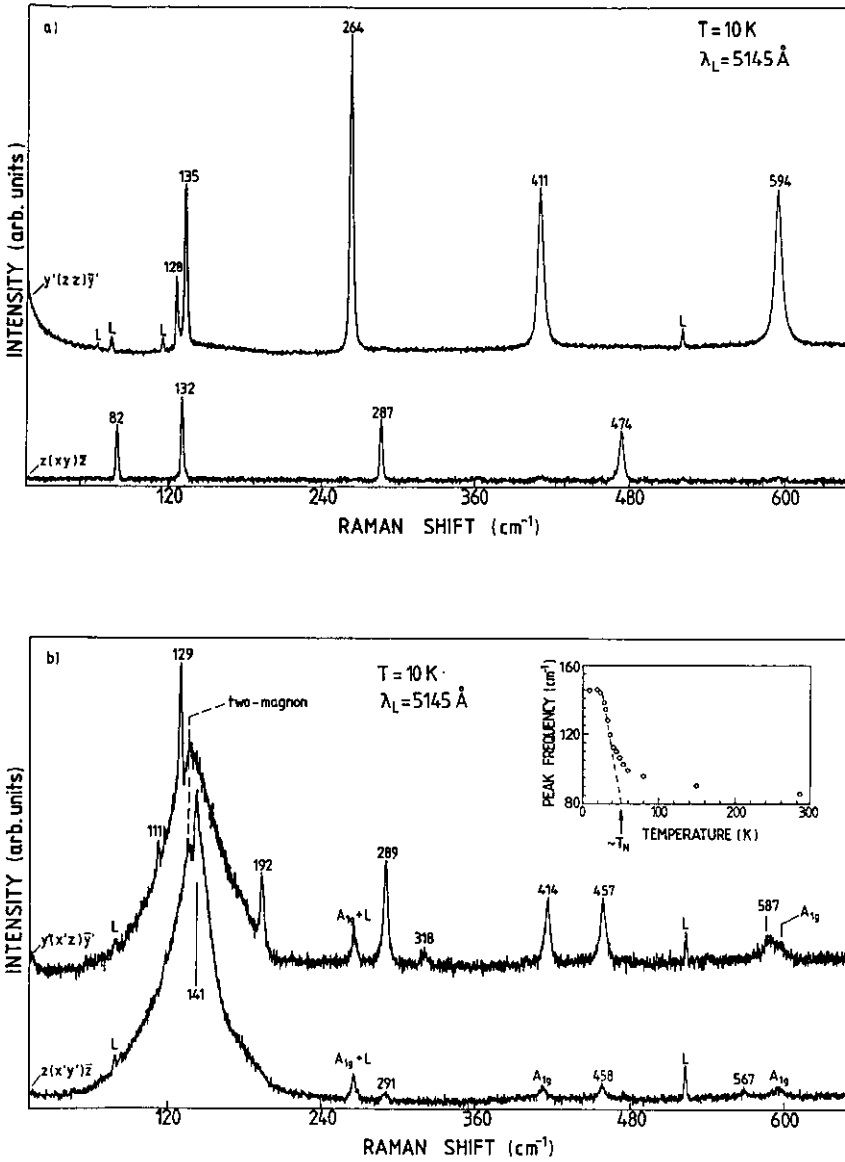
Figure 3. (a) Raman scattering spectra of Bi_2CuO_4 single crystals at 10 K for $y'(zz)\bar{y}'$ and $z(xy)\bar{z}$ polarizations; (b) the same spectra for $y'(x'z)\bar{y}'$ and $z(x'y')\bar{z}$ polarizations ($x \parallel [100]$, $y \parallel [010]$, $z \parallel [001]$, $x' \parallel [110]$ and $y' \parallel [1\bar{1}0]$).

are given in [5] and we shall not repeat them here. We recall that the lowest-frequency modes of A_{1g} and B_{2g} symmetry originate from Bi atom vibrations while the A_{1g} mode at 135 cm^{-1} originates from translational vibrations of the CuO_4 planes along z axes. The remaining A_{1g} and B_{2g} modes of higher frequency correspond to the vibrations of the oxygen atoms as already discussed in [5].

The $x'z$ and $x'y'$ polarized spectra with E_g and B_{1g} Raman-active modes are presented in figure 3(b). It has already been shown [5] that the intensity of B_{1g}
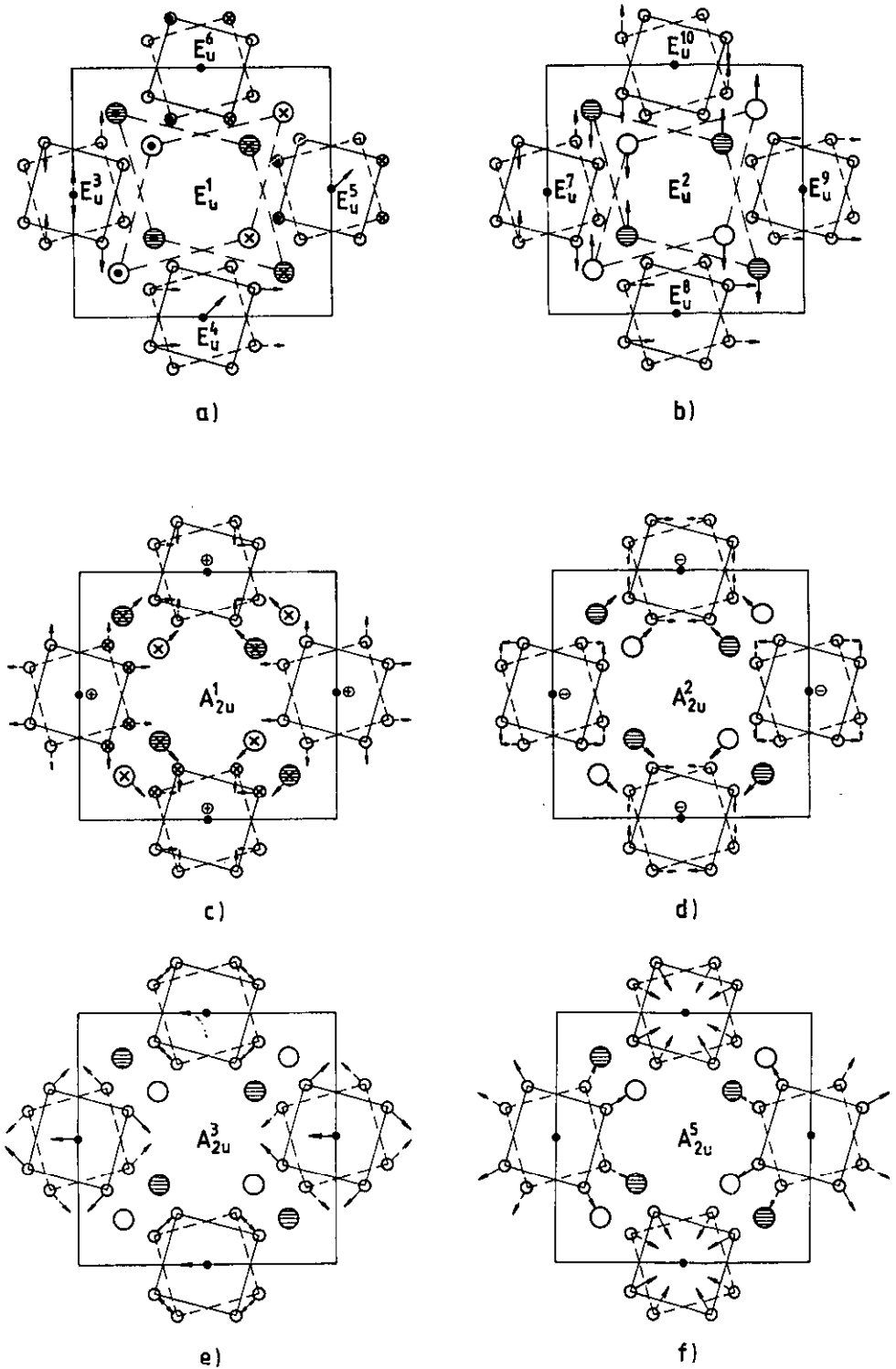
Figure 4. Normal-mode displacements of Bi_2CuO_4 for (*a*), (*b*) E_u and (*c*)–(*f*) A_{2u} infrared-active modes.

symmetry modes is approximately 100 times lower than the intensity of the B_{2g} modes, which explains why they were not observed until now. The Raman spectra with B_{1g} symmetry, presented in figure 3(b), were obtained as the average value of 30 successive recorded spectra which increased the signal-to-noise ratio and made the B_{1g} modes visible. We assigned the modes at 141, 291, 458 and 567 cm^{-1} as B_{1g} modes. Besides these modes, several laser plasma lines as well as the 'leakage' of the A_{1g} modes are observed. Also, one wide feature in figure 3(b), centred at around 137 cm^{-1}, becomes dominant at temperatures below $T_N = 45$ K (paramagnetic-to-antiferromagnetic phase transition temperature in Bi$_2$CuO$_4$). The peak frequency dependence of this mode (inset in figure 3(b)) leads us to conclude that this excitation can be assigned as a two-magnon mode. More detailed analysis of the light scattering on magnetic excitations of Bi$_2$CuO$_4$ can be found in [6].

In the case of E_g symmetry, eight modes were observed from 11 modes predicted by FGA. All the mode frequencies are collected in table 1. The normal-mode displacements for some of these modes are given in [5]. The dominant mode in this polarization at 10 K also arises from two-magnon scattering.

Let us once again consider figure 1 in which Bi$_2$CuO$_4$ infrared spectra are shown. As already discussed [5], infrared-active modes with frequencies below 100 cm^{-1} and above 400 cm^{-1} arise from the vibrations of bismuth and oxygen atoms, respectively.

The normal coordinate calculation [9] was performed for detailed analysis of these modes (figure 4). The first two E_u modes (E_u^1 and E_u^2) at about 38 and 91 cm^{-1} originate from vibrations of bismuth atoms along the z axis and from bond-bending in-plane vibrations of Bi atoms as illustrated in figures 4(a) and (b), respectively. The next two modes at about 150 and 196 cm^{-1} originate from translational vibrations of Cu and oxygen atoms in the CuO$_4$ plane (figure 4(a)) while a mode at 218 cm^{-1} (E_u^5) arises from out-of-phase vibrations of oxygen atoms in CuO$_4$ planes which tend to 'rotate' the CuO$_4$ chain. The infrared modes at higher frequencies E_u^6 to E_u^{10}) originate dominantly from translational vibrations of oxygen atoms in CuO$_4$ squares (see figure 4(b)).

Normal-mode displacements of Bi$_2$CuO$_4$ for A_{2u}-symmetry infrared-active modes are shown in figures 4(c)–(f). The modes at frequencies of 100 and 130 cm^{-1} are due to collective vibrations of Bi and Cu atoms with a small contribution from oxygen atoms as illustrated in figures 4(c) and (d). The A_{2u}^3 mode originates from vibrations of oxygen atoms which rotate two stacked CuO$_4$ squares in opposite directions plus translational vibrations of the Cu atoms along the x axis (figure 4(e)) while the A_{2u}^4 mode has the same normal-mode displacement as the A_{2u}^3 mode but without vibrations of the Cu atoms. Finally, the A_{2u} mode with the highest frequency at TO of 560 cm^{-1} is a breathing mode of the isolated CuO$_4$ squares (figure 4(f)). The dipole orientation of this mode lies in the (001) plane and gives a small contribution in the $E \parallel c$ polarization. This is in agreement with the spectra given in figure 1(b) which shows that the reflection coefficient of this mode is only 8%. More detailed analysis of the vibrational properties of Bi$_2$CuO$_4$ involving lattice dynamic calculations is in progress.

References

[1] Boivin J C, Trehoux J and Thomas D 1976 *Bull. Soc. Fr. Minéral. Cristallogr.* **99** 193
[2] Sreedhar K, Ganghyly P and Ramasesha R 1988 *J. Phys. C: Solid State Phys.* **21** 1129
[3] Troc R, Janicki J, Filatow I, Fischer P and Murasik A 1990 *J. Phys.: Condens. Matter* **2** 6989
[4] Yamada K, Takada K, Hosoya S, Watanabe Y, Endoh Y, Tomonaga N, Suzuki T, Ishigaki T, Kamijama T, Asano H and Izumi F 1991 *J. Phys. Soc. Japan* **20** 2406
[5] Popović Z V, Kliche G, Cardona M and Liu R 1990 *Phys. Rev.* B **41** 3824
[6] Konstantinović M J, Popović Z V, Dević S D, Revcolevschi A and Dhalenne G 1992 *J. Phys.: Condens. Matter* **4** 7913
[7] Dhalenne G, Revcolevschi A, Ain M, Hennion B, Andre G and Parette G 1991 *Cryst. Prop. Prep.* **36** 11
[8] Popović Z V, Thomsen C, Cardona M, Liu R, Stanišić G, Kremer R and König W 1988 *Solid State Commun.* **66** 965
[9] Kliche G unpublished